Robotica (2006) volume 24, pp. 549–555. © 2006 Cambridge University Press
doi:10.1017/S0263574705002602 Printed in the United Kingdom

Forward kinematic solution and its applications for a 3-DOF parallel kinematic machine (PKM) with a passive link

Z. M. Bi* and S. Y. T. Lang

Integrated Manufacturing Technologies Institute, National Research Council, London, ON, Canada, N6G 4X8

(Received in Final Form: November 27, 2005. First published online: February 15, 2006)

SUMMARY

In this paper, a 3-DOF parallel kinematic machine (PKM) with a passive link is introduced. The forward kinemaic model is established, and a new technique is proposed to solve this model. The developed forward kinematic solver (FKS) is employed in two new applications: the determination of joint workspace and sensor-based real-time monitoring. A *joint workspace* concept is proposed for the optimization of a PKM structure. It is defined as a reachable area in the joint coordinate system under given ranges of active joint motions. The larger a joint workspace is, the higher utilization of joint motion capacity is. Sensor-based monitoring is applied in real-time system operation, by which a remote user can monitor a PKM through Internet based on the feedbacks of the joint encoders or the on-site stereo camera.

KEYWORDS: Parallel Kinematic Machine (PKM); Forward kinematics; Joint workspace; Sensor-based monitoring; Web-based control; Java3D

I. INTRODUCTION

Forward kinematics finds the end-effector motion when the joint motions of a robot are given. A Parallel Kinematic Machine (PKM) includes closed-loop chains that bring challenges to solve its forward kinematic problem. Either a dedicated approach or a general approach can be applied for solving forward kinematics. *A dedicated approach* works only for a specified PKM type; all of the structural characteristics can be utilized to obtain a concise solution and simplify a solving procedure. *A general approach* is applicable to a PKM family with some common characteristics; it usually needs iterative algorithms to obtain the solutions finally. Many researchers have studied forward kinematic problems of the PKMs,[1–7] but very few of them targeted certain PKM families. Note that it is impossible to develop a universal approach applicable to all of the PKMs. Moreover, a general approach needs to deal with all of the possibilities a PKM topology can be, the more general the approach is, the more cumbrous the solver will be.[8] In the course of developing new PKMs, a dedicated approach is still the first choice. Therefore, further work on forward kinematics will be required as long as new PKMs are proposed continuously. In this paper, forward kinematics of our newly developed 3-DOF PKM will be studied.

The benefits of a forward kinematic solver (FKS) have not been totally explored. Since forward kinematics is not essential to designing and applying a PKM system; the application of a PKM is usually task-oriented, and simple inverse kinematics can address most of the design and application issues satisfactorily. However, there is no doubt that well-understanding of forward kinematics is beneficial to the structural optimization and the implementation of the control and monitoring in some extensive areas. We will discuss two new applications of a FKS: determination of joint workspace and sensor-based monitoring.

Design concepts of a PKM must be evaluated in terms of many design criteria.[9–17] Among these criteria, workspace is one of the most primary considerations. Workspace is traditionally measured for the end-effector motion in Cartesian coordinate system. Workspace can also be measured for active joint motions in joint coordinate system as well. *Joint workspace* is defined as the volume of the workspace in the joint coordinate system.[18] It has attracted little attention because most of the industrial robots are serial, and their joints are active which can reach their entire motion domains. However, for a PKM or hybrid robot, some or all joints can not reach the entire motion domains because of the closed-loop constraints. Note that a robot is functioned to transform joint motions to the end-effector motion; the utilization of joint motion capacity will be seriously restricted for a PKM or hybrid robot. No work has been conducted to analyze the joint workspace of a PKM,[9] and none criterion is available to evaluate the utilization of the joint motion capacity.

Sensor-based monitoring is very useful when the machine operator/user has to control and monitor a machine in a remote or distributed environment. The situations become more and more popular in distributed manufacturing, dangerous environments, and military operations. Some sensor-based systems have been developed for robotic applications,[19–26] but none of them use a FKS for a PKM. The benefits of a FKS for sensor-based monitoring will be discussed in Section V.

In this paper, forward kinematics of a new PKM will be studied. Two new applications of the FKS will be illustrated. The remainder of the paper will be organized as follows: Section II introduces the 3-DOF PKM system with a passive link, and presents its parametrical description. Section III develops the forward kinematic model, and introduces a new

* **Corresponding author**. E-mail: Zhuming.Bi@nrc-cnrc.gc.ca

approach for solving this model. Sections IV and V provide two new applications of the FKS. Section IV illustrates the concept of joint workspace, and illustrates how the FKS is used to calculate the joint workspace of a PKM. Section V develops a sensor-based monitoring system; the system architecture is described. Section VI concludes this paper's contributions.

II. A 3-DOF PKM WITH A PASSIVE LINK

II.1. Motivation

Various PKMs have been developed at the National Research Council Canada[26–30], the most interesting one is the tripod system with 3-DOF, since a PKM with three or less DOF are adequate for many applications, and it can be combined with other flexible devices for more DOFs. However, the previous version of the tripod system has two unsolved problems: (i) system stiffness is not high enough to compete in the high-speed machining; and (ii) the system produces the coupled motions. In our application, the operation requires x and y rotations and z translation, but the system has the coupled z rotation and x and y translations. These coupled motions have to be compensated.

To address the aforementioned problems, a new tripod system is designed. As shown in Figure 1, the new system has three symmetrical active links and a passive link. It is similar to the Tricept system,[7,26] but it is fundamentally different in sense that: (i) the active links are connected to the end-effector platform by spherical joints; (ii) the universal joint of the passive link is located on the end-effector platform rather than on the base platform. As a result, the x and y translations and the z rotation at the reference O_e are eliminated completely; (iii) the new system is applied for the end-effector motion with x and y rotations and z translation.

II.2. Parametric description

The structure of the new system is shown in Figure 1. It has three platforms: base platform $B_1B_2B_3$, middle platform $M_1M_2M_3$, and end-effector platform $E_1E_2E_3$. The base platform is fixed on the ground. The middle platform is used to support guide-way B_iM_i of active link D_iE_i. The end-effector platform is used to mount a machine tool. The passive link is installed between the middle platform and the end-effector platform. Active link D_iE_i is connected to the end-effector platform by a spherical joint at E_i, and to the slide of the active prismatic joint by a universal joint at D_i. The passive link is fixed on the middle platform at one end, and connected to the end-effector platform by a universal joint at the other end.

The following parameters can be used to describe this tripod PKM:

(i) the angle α_i (i = 1, 2, 3) between O_bB_i and $\boldsymbol{x}_b$
(ii) the angle β_i (i = 1, 2, 3) between O_eE_i and $\boldsymbol{x}_e$
(iii) the size of the base platform l_b,
(iv) the size of the end-effector platform l_e,
(v) the direction of a guide-way γ, and
(vi) the length of an active link l_i.

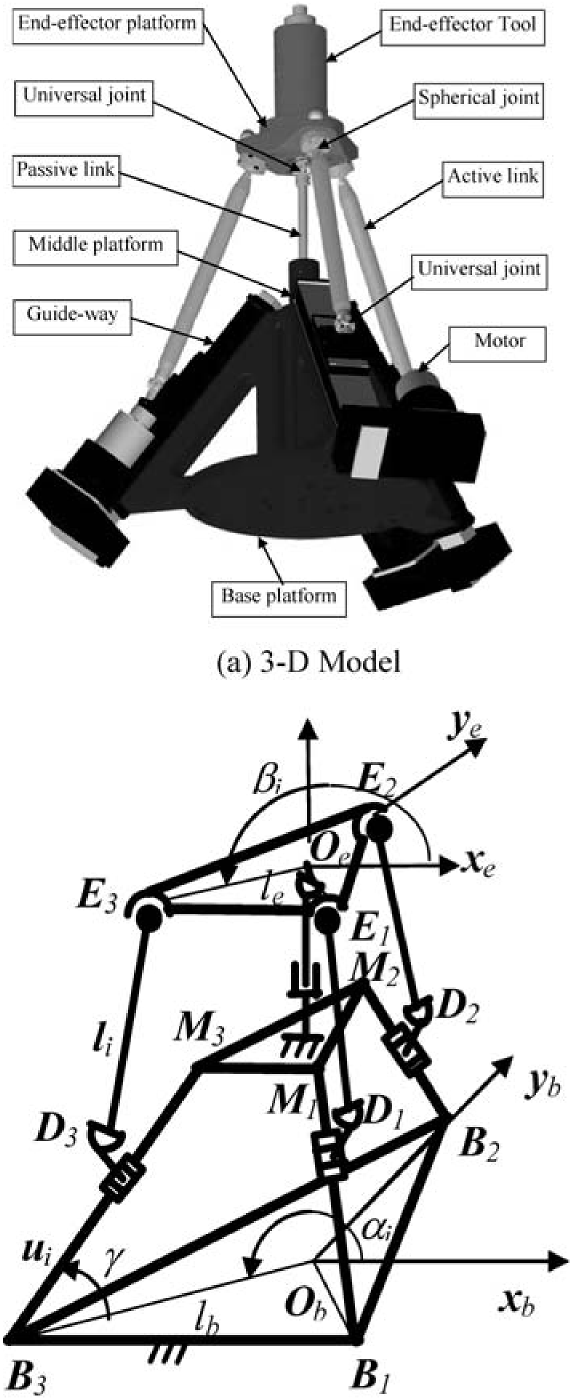

(a) 3-D Model

(b) Parametric Model

Fig. 1. A 3-DOF tripod with a passive link.

III. FORWARD KINEMATIC MODEL AND ITS SOLUTION

In Figure 1b, to formulate a forward kinematic problem, two coordinate systems, $\{O_e—\boldsymbol{x}_e\boldsymbol{y}_e\boldsymbol{z}_e\}$ and $\{O_b—\boldsymbol{x}_b\boldsymbol{y}_b\boldsymbol{z}_b\}$, are established on the end-effector platform and the base platform, respectively. $\{O_e—\boldsymbol{x}_e\boldsymbol{y}_e\boldsymbol{z}_e\}$ is dealt with the world coordinate system.

III.1. End-effector motion and joint motions

Forward kinematics finds the end-effector motion when the active joint motions of a PKM are given. In Figure 1, active

https://doi.org/10.1017/S0263574705002602 Published online by Cambridge University Press

joint motions are given and denoted by u_i (i = 1, 2, 3). The end-effector motion will be described by three rotational parameters $(\theta_x, \theta_y, \theta_z)$ and three translational parameters (x_e, y_e, z_e),

$$T_e^b = \begin{bmatrix} R_e & p_e^b \\ 0 & 1 \end{bmatrix}$$

$$= \begin{bmatrix} c\theta_y c\theta_z & -c\theta_y s\theta_z & s\theta_y & x_e \\ s\theta_x s\theta_y c\theta_z + c\theta_x s\theta_z & -s\theta_x s\theta_y s\theta_z + c\theta_x c\theta_z & -s\theta_x c\theta_y & y_e \\ -c\theta_x s\theta_y c\theta_z + s\theta_x s\theta_z & c\theta_x s\theta_y s\theta_z + s\theta_x c\theta_z & c\theta_x c\theta_y & z_e \\ 0 & 0 & 0 & 1 \end{bmatrix} \tag{1}$$

where

T_e^b is the end-effector motion array with respect to $\{O_b$-$\mathbf{x}_b\mathbf{y}_b\mathbf{z}_b\}$.

R_e and p_e^b represent the orientation and the position of the end-effector platform, respectively.

c and s represent the cosine and sine functions, respectively.

The passive link is connected to the end-effector platform by a universal joint at O_e. Therefore, x and y translations and z rotation are eliminated at O_e, i.e. $(x_e = y_e = 0, z_\theta = 0)$. The end-effector motion can be simply denoted by $(\theta_x, \theta_y, z_\theta)$, where θ_x and θ_y are x and y rotations, and z_e is z translation. The end-effector motion array is simplified as

$$T_e^b = \begin{bmatrix} R_e & p_e^b \\ 0 & 1 \end{bmatrix} = \begin{bmatrix} c\theta_y & 0 & s\theta_y & 0 \\ s\theta_x s\theta_y & c\theta_x & -s\theta_x c\theta_y & 0 \\ -c\theta_x s\theta_y & s\theta_x & c\theta_x c\theta_y & z_e \\ 0 & 0 & 0 & 1 \end{bmatrix} \tag{2}$$

Till now, there is no direct relation between the joint motions and the end-effector motion. In the next section, the structural constraints of the PKM are further considered to build their relations.

III.2. Closed-loop constraints

Three active links are connected to the end-effector platform simultaneously. It results in the geometric constraints of the PKM. These constraints define the relations between the joint motions and the end-effector motion.

As shown in Figure 2, the PKM includes three independent kinematic chains $O_bO_eE_iD_iB_i$ $(i = 1, 2, 3)$. The following geometric constraints can be identified from these chains:

$$|O_bE_i - O_bB_i - B_iD_i| = |D_iE_i| \quad (i = 1, 2, 3) \tag{3}$$

O_bE_i relates to the end-effector motion $(\theta_x, \theta_y, z_\theta)$ as,

$$O_bE_i = R_e^b \begin{bmatrix} l_e c\beta_i \\ l_e s\beta_i \\ z_0 \end{bmatrix} + p_e^b$$

$$= \begin{bmatrix} l_e c\beta_i c\theta_y + z_0 s\theta_y \\ l_e c\beta_i s\theta_x s\theta_y + l_e s\beta_i c\theta_x - z_0 s\theta_x c\theta_y \\ -l_e c\beta_i c\theta_x s\theta_y + l_e s\beta_i s\theta_x + z_e + z_0 c\theta_x c\theta_y \end{bmatrix} \tag{4}$$

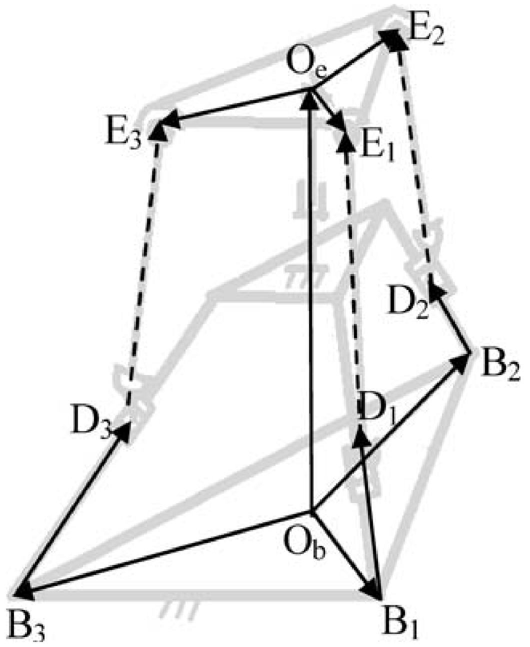

Fig. 2. Closed-loop constraints of the PKM.

where z_0 is the offset of spherical joints along z axis.

O_bD_i relates to the joint motions as,

$$O_bD_i = O_bB_i + B_iD_i = \begin{bmatrix} (l_b - u_i c\gamma)c\alpha_i \\ (l_b - u_i c\gamma)s\alpha_i \\ u_i s\gamma \end{bmatrix} \tag{5}$$

The active link D_iE_i has a fixed-length, substituting eq. (4) and (5) into (3) gives,

$$\left.\begin{matrix} z_e^2 + (A_i c\theta_y + B_i s\theta_y + C_i)z_e + (D_i c\theta_y + E_i s\theta_y + F_i) = 0 \\ (i = 1, 2, 3) \end{matrix}\right\} \tag{6}$$

where the coefficients $A_i \sim F_i$ are related to u_i and θ_x, and expressed by

$$\begin{aligned} A_i &= 2z_0 c\theta_x \\ B_i &= -2l_e c\beta_i c\theta_x \\ C_i &= 2l_e s\beta_i s\theta_x - 2u_i s\gamma \\ D_i &= 2l_e u_i c\alpha_i c\beta_i c\gamma - 2l_e l_b c\beta_i c\alpha_i + 2z_0 l_b s\alpha_i s\theta_x \\ &\quad - 2z_0 u_i\,(s\alpha_i c\gamma s\theta_x + s\gamma c\theta_x) \\ E_i &= -2z_0 l_b c\alpha_i + 2z_0 u_i c\alpha_i c\gamma - 2l_e l_b s\alpha_i c\beta_i s\theta_x \\ &\quad + 2l_e u_i\,(s\alpha_i c\beta_i c\gamma s\theta_x + c\beta_i s\gamma c\theta_x) \\ F_i &= l_e^2 + l_b^2 + z_0^2 + u_i^2 - l_i^2 \\ &\quad - 2\,(l_e s\beta_i\,(u_i s\gamma s\theta_x + (l_b - u_i c\gamma)\,s\alpha_i c\theta_x) + l_b u_i c\gamma) \end{aligned}$$

III.3. Forward kinematic model

Eq. (6) expresses the dependences of the joint motions and the end-effector motion, while joint motions u_i $(i = 1, 2, 3)$ are known, and the end-effector motion $(\theta_x, \theta_y, z_\theta)$ is unsolved.

https://doi.org/10.1017/S0263574705002602 Published online by Cambridge University Press

The strategy to build a forward kinematic model is to decouple the unknown parameters $(\theta_x, \theta_y, z_\theta)$, so that each equation of eq. (6) only relates to one of these parameters.

By subtracting one equation from another in eq. (6) yields,

$$\left.\begin{array}{r}(A_{ij}z_e + D_{ij})c\theta_y + (B_{ij}z_e + E_{ij})s\theta_y + C_{ij}z_e + F_{ij} = 0\\ (i \neq j)\end{array}\right\} \tag{7}$$

where

$$\begin{array}{l}A_{ij} = A_i - A_j,\, B_{ij} = B_i - B_j,\, C_{ij} = C_i - C_j\\ D_{ij} = D_i - D_j,\, E_{ij} = E_i - E_j,\, F_{ij} = F_i - F_j\end{array}$$

The purpose of eq. (7) is to eliminate the items of z_e^2. The dependence of θ_y on z_e and θ_x are found as,

$$\left.\begin{array}{l}c\theta_y = -\big(Gz_e^2 + Hz_e + I\big)/(Jz_e + K)\\ s\theta_y = -(Lz_e + M)/(Jz_e + K)\end{array}\right\} \tag{8}$$

where the coefficients $F \sim L$ relate only to θ_x,

$$\begin{array}{l}G = B_{12}C_{13} - B_{13}C_{12}\\ H = B_{12}F_{13} + C_{13}E_{12} - B_{13}F_{12} - C_{12}E_{13}\\ I = E_{12}F_{13} - E_{13}F_{12}\\ J = B_{13}D_{12} - B_{12}D_{13}\\ K = D_{12}E_{13} - D_{13}E_{12}\\ L = C_{12}D_{13} - C_{13}D_{12}\\ M = D_{13}F_{12} - D_{12}F_{13}\end{array}$$

Further, θ_y must satisfy the formula $c^2\theta_y + s^2\theta_y = 1$; substituting eq. (8) into it gives,

$$M_4z_e^4 + M_3z_e^3 + M_2z_e^2 + M_1z_e + M_0 = 0 \tag{9}$$

where

$$\begin{array}{l}M_4 = G^2\\ M_3 = 2GH\\ M_2 = H^2 + L^2 - J^2 + 2GI\\ M_1 = 2(HI + LM - KJ)\\ M_0 = I^2 + M^2 - K^2\end{array}$$

Note that eq. (6) has three independent equations. Eq. (8) uses two of them, the remainder one can be derived by substituting eq. (8) into any one of the equations in eq. (6). Assume $i = 1$, one gets,

$$N_3z_e^3 + N_2z_e^2 + N_1z_e + N_0 = 0 \tag{10}$$

where

$$\begin{array}{l}N_3 = J + A_1G\\ N_2 = C_1J + K + A_1H + D_1G + B_1L\\ N_1 = F_1J + C_1K + A_1I + D_1H + E_1L + B_1M\\ N_0 = F_1K + D_1I + E_1M\end{array}$$

A feasible solution z_e has to satisfy eq. (9) and (10) simultaneously. Based on Bezout's method,[3,5,6] the coefficients of these equations must satisfy the following condition,

$$\Delta = \begin{vmatrix} M_4 & M_3 & M_2 & M_1 & M_0 & 0 & 0\\ 0 & M_4 & M_3 & M_2 & M_1 & M_0 & 0\\ 0 & 0 & M_4 & M_3 & M_2 & M_1 & M_0\\ N_3 & N_2 & N_1 & N_0 & 0 & 0 & 0\\ 0 & N_3 & N_2 & N_1 & N_0 & 0 & 0\\ 0 & 0 & N_3 & N_2 & N_1 & N_0 & 0\\ 0 & 0 & 0 & N_3 & N_2 & N_1 & N_0 \end{vmatrix} = 0 \tag{11}$$

Eq. (11) is an equation about θ_x when joint motions u_i $(i = 1, 2, 3)$ are given.

III.4. Solution to forward kinematic model

The strategy to solving forward kinematic model is straightforward: (i) to calculate θ_x from eq. (11), (ii) to calculate z_e from eq. (10), and (iii) to calculate θ_y from eq. (8). Here, an efficient and reliable technique is introduced.

Assume the following standard transformations are applied,

$$t = \tan(\theta_x/2),\ c\theta_x = (1 - t^2)/(1 + t^2),\ s\theta_x = 2t/(1 + t^2) \tag{12}$$

Eq. (11) turns into a polynomial equation with the order of 24. The order can be estimated from the representations of the coefficients in eq. (9) and (10). However great challenge can arise to determine total 25 coefficients of the polynomial equation symbolically, since the substitution of triangular transformation eq. (12) into eq. (11) is very trivial and error-prone. The following procedure calculates these coefficients numerically.

After eq. (11) is converted by the standard transformation eq. (14), it becomes,

$$\sum_{i=0}^{i=24} k_i t^i = \Delta \cdot (1 + t^2)^{12} \tag{13}$$

where k_i $(i = 0, 1, \ldots 24)$ only relate to joint motions u_i $(i = 1, 2, 3)$ and the structural parameters of the PKM.

When joint motions u_i $(i = 1, 2, 3)$ are given, a set of 25 linear equations about k_i $(i = 0, 1, \ldots 25)$ can be produced by assigning θ_x with 25 different values in eq. (11). The coefficients can be dealt with the design variables of this equation set, and then be calculated easily via some linear algorithms.

A numerical algorithm can be applied to get all of the roots about θ_x from the polynomial equation. After θ_x is calculated from the polynomial equation, z_e and θ_y can be calculated from eq. (10) and (8), sequentially. Finally, O_bE_i are determined from eq. (4), and the end-effector motion

https://doi.org/10.1017/S0263574705002602 Published online by Cambridge University Press

array is obtained as,

$$T_e = \begin{bmatrix} \boldsymbol{R}_e & \boldsymbol{p}_e^b \\ 0 & 1 \end{bmatrix} = \begin{bmatrix} (O_bE_1 - O_bE_3)/(\sqrt{3}l_e) & (O_bE_2 - O_bO_e)/l_e & (O_bE_1 - O_bE_3) \times (O_bE_2 - O_bO_e)/\left(\sqrt{3}l_e^2\right) & O_bO_e \\ 0 & 0 & 0 & 1 \end{bmatrix} \tag{14}$$

where

T_e and R_e correspond to the terms in eq. (2),

O_bE_i is determined from eq. (4) when the end-effector motion is known, and

$O_bO_e = (O_bE_1 + O_bE_2 + O_bE_3)/3.0.$

IV. APPLICATION I — JOINT WORKSPACE

In this section, the FKS is applied to calculate joint workspace. *Joint workspace* is the set of points in the joint coordinate system that a robot can reach. In contrast, the concept of the workspace, which has been defined as the set of points the robot can reach in the task space, is called *task workspace*.

A robot is functioned to transform the joint motions into the end-effector motion. A good robotic design achieves high efficiency of this motion transformation. Task workspace can only evaluate the volume of the working area with respect to the Cartesian space; it cannot evaluate how well the joint motions span this task space. To evaluate the transform efficiency appropriately, the concept of joint workspace is utilized.

For a hybrid or parallel robot with a closed-loop structure, a configuration should satisfy a set of the geometric constraints, and the capability of robotic joints can be restricted because of these constraints. The significance of joint workspace concept includes: (i) evaluating how well the joint motions are transformed into the end-effector motion, (ii) justifying weather or not a configuration with a set of the joint motions is feasible, and (iii) optimizing the structural parameters when the trajectory of the task is specified as design constraints and the system is designed to fulfill this task efficiently.

A particular application of joint workspace is out of the scope of the paper. However, the following example illustrates how the FKS is used to calculate joint workspace and how well the joint motions are utilized to span task workspace.

In Table I, structural parameters of the PKM prototype have been optimized with consideration of task workspace, geometric constraints of joints modules, and system stiffness.

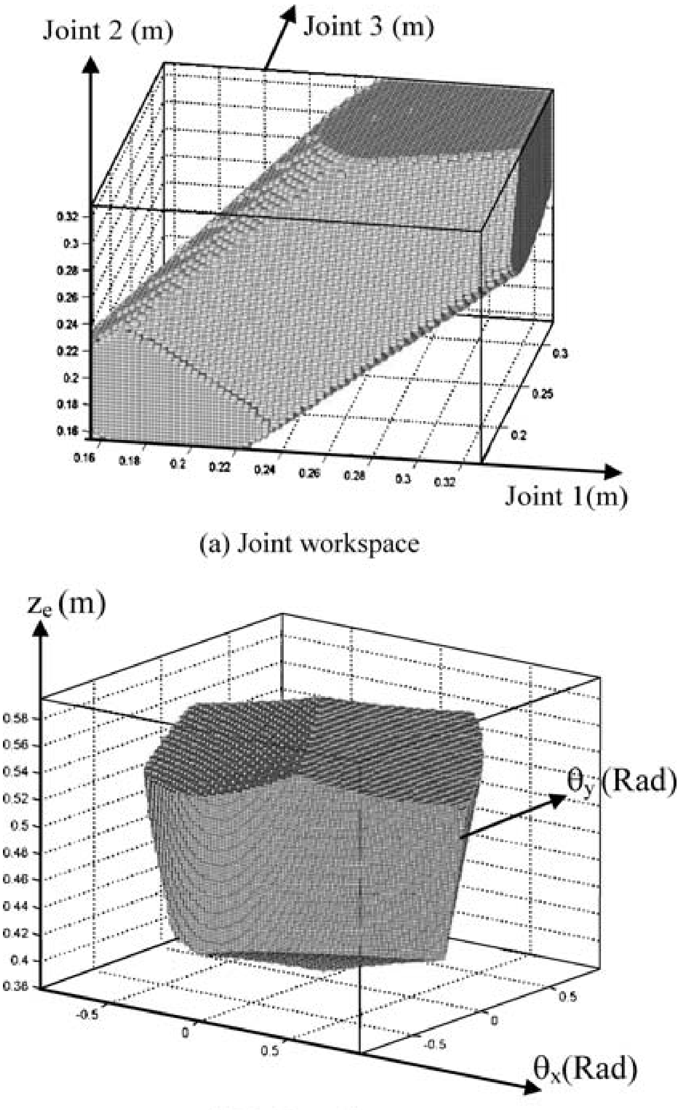

(a) Joint workspace

(b) Task workspace

Fig. 3. Workspace for the PKM Prototype.

Table I. Structural parameters of the PKM prototype.

Structural Parameters	α_i			β_i						
	α_1	α_2	α_3	β_1	β_2	β_3	γ	l_b	l_e	l_i
	−30°	0°	−120°	−30°	0°	−120°	50°	0.341 m	0.08 m	0.377 m
Joint Parameters	Prismatic joints			Spherical joints			Universal joints for active links		Universal joints for passive link	
	Active			Passive			Passive		Passive	
	(0.124 m, 0.324 m)			(−45°, 45°)			(−50°, 50°)		(−50°, 50°)	

https://doi.org/10.1017/S0263574705002602 Published online by Cambridge University Press

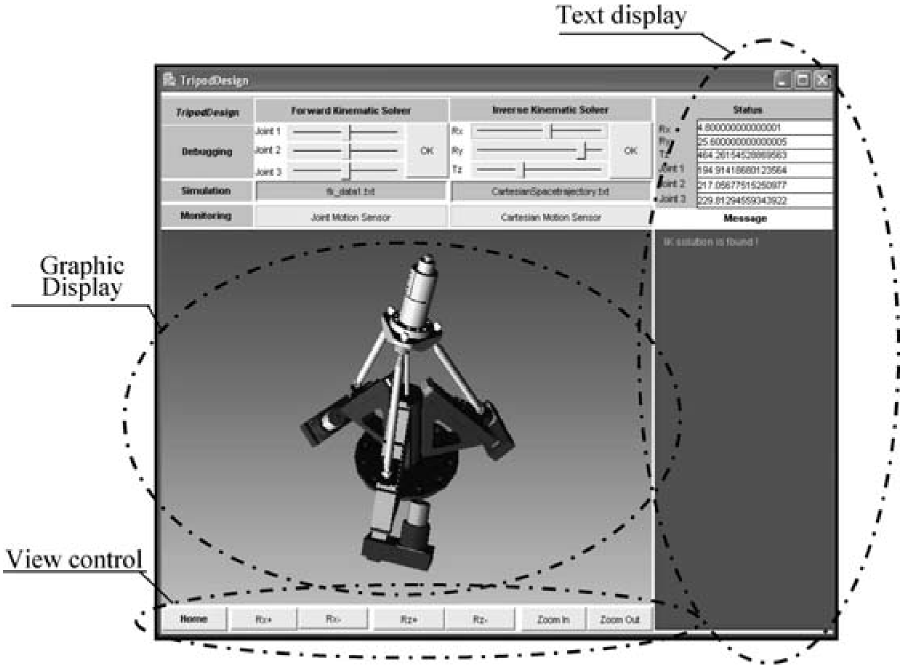

fk_data1.txt

CartesianSpacetrajectory.txt

Rx 4.800000000000001

Ry 25.600000000000005

Tz 464.26154528869563

Joint 1 194.91418680123564

Joint 2 217.05677515250977

Joint 3 229.81294559343922

IK solution is found !

Fig. 4. Sensor-based debugging, simulation, and monitoring environment.

To calculate the joint workspace, firstly, a joint coordinate system is configured by joint motions of three active joints, and the boundaries of the joint workspace are determined by the limits of these joint motions. Secondly, the entire area with the boundaries is discritized and each unit is represented by the coordinates of its centre. Thirdly, forward kinematics is solved for each unit. If the solution exists, this unit locates within the joint workspace. Fourthly, the joint workspace is an assembly of all of the units whose forward kinematic solution exists.

The joint workspace of the given PKM prototype is shown in Figure 3a, and the corresponding task workspace is shown in Figure 3b, Only 55 percentage of the entire motion domain has feasible forward kinematic solution. Note that for a serial robot, 100 percentage of joint workspace can be reached unless the components of the robot have self-interference. From the viewpoint of the efficiency of the motion transformation, the design needs improving.

V. APPLICATION II — SENSOR-BASED MONITORING

In this section, the FKS is applied in sensor-based monitoring. Many web-based control, simulation, and monitoring systems have been introduced.[19–26] The methodologies of system development have been well established. However, the challenge of a new application is to build customized system behavior models related to sensor feedbacks. In this sense, the majority of available systems have targeted the serial robots with simple kinematics, and none of them utilize the forward kinematic solutions of PKMs. With the FKS, only the encoder feedbacks of the active joints are needed for graphical animation of machine operations, both of sensors hardware and data communication can be minimized.

The other issue in our application is the integration of the programs from heterogonous environments. The FKS has been developed in Matlab, in order that powerful capacities of mathematic operations of the Matlab can be fully accessed. Real-time control and data acquisition are developed in C++, and the graphical simulation and GUI are developed in Java 3D. Sensor-based simulation and monitoring system have integrated all of these heterogonous programs. In particular, Jmatlink is used to call the Matlab program from Java.[31]

Figure 4 shows the user interfaces of the integrated environment. The environment includes the debugging module, simulation module, and monitoring module. The tripod PKM system can be debugged by changing system parameters interactively. The simulation can be driven by a trajectory given either in the Cartesian or joint coordinate systems. The monitoring module works in two modes. One is based on encoder feedbacks, and the other is based on the feedback of camera in the Cartesian space. The environment allows a user to change the view of graphic display interactively, and it also displays text message in real-time system operation.

VI. CONCLUSIONS

A newly developed 3-DOF tripod PKM has been introduced. The PKM can produce the pure 3-DOF motion of x and y rotations and z translation, while the coupled x and y translations and z rotation are eliminated. The forward kinematic model is mainly discussed. It turns out a polynomial equation with the order of 24. New technique is introduced to solve this forward kinematic model numerically. The significance of the new technique is to eliminate the trivial and error-prone symbolic derivation of the coefficients in solving the polynomial equation

https://doi.org/10.1017/S0263574705002602 Published online by Cambridge University Press

with a high order. Two new applications of the FKS are proposed. The first one is for studying joint workspace. The concept of joint workspace is proposed to evaluate the PKM performance from the viewpoint of the efficiency of the motion transformation. It is very meaningful for the design of a robot with a closed-loop or hybrid structure. The other application is for sensor-based monitoring. The FKS of a PKM is firstly applied in contrast to other similar systems for robotic applications; moreover, both of the sensors hardware and the data communication can minimized.

References

1. J-P. Merlet, "Direct kinematics and assembly modes of parallel manipulators", *Int. J. Robotics Research* **11**. No. 2, 150–162 (1992).
2. J-P. Merlet, "Direct kinematics of parallel manipulators", *IEEE Trans. on Robotics and Automation* **9**, No. 6, 842–845 (1993).
3. C. Gosselin and J-P. Merlet, "On the direct kinematics of planar parallel manipulators: special architectures and number of solutions", *Mechanism and Machine Theory* **29**, No. 8, 1083–1097 (1994).
4. Carlos Vombin, Lluis Ros and Federico Thomas, "On the computation of the direct kinematics of parallel spherical mechanisms using Bernstein polynomials", *Proceedings of the 2001 IEEE International Conference on Robotics and Automation*, Seoul, Korea (May 21–26, 2001) pp. 3332–3337.
5. C. M. Gosselin, J. Sefrioui and M. J. Richard, "On the direct kinematics of spherical three-degree-of-freedom parallel manipulators of general architecture", *ASME Journal of Mechanical Design* **116**, 594–598 (1994).
6. C. M. Gosselin, J. Sefrioui and M. J. Richard, "On the direct kinematics of spherical three-degree-of-freedom parallel manipulators with a coplanar platform", *ASME Journal of Mechanical Design* **116**, 585–593 (1994).
7. Bruno Siciliano, "The Tricept robot: Inverse kinematics, manipulability analysis and closed-loop direct kinematics algorithm", *Robotica* **17**, Part 4, pp. 437–445 (1999).
8. Z. M. Bi, On Adaptive Robot Systems for Manufacturing Applications, *Doctorial Thesis* (University of Saskatchewan, Saskatoon, Canada, 2002).
9. A. Kumar and K. J. Waldron, "The workspaces of a mechanical manipulator", *ASME Journal of Mechanical Design* **103**, 665–672 (1981).
10. K. C. Gupta and B. Roth, "Design considerations for manipulator workspace", *ASME Journal of Mechanical Design* **104**, 704–711 (1982).
11. Z. C. Lai and C. H. Meng, "The dexterous workspace of simple manipulators", *IEEE Journal of Robotics and Automation* **4**, No. 1, 99–103 (1988).
12. D. C. H. Yang and Z. C. Lai, "On the dexterity of robotic manipulators – service angle", *ASME Journal of Mechanism, Transmissions, Automation and Design* **107**, 262–270 (1985).
13. F. C. Park and R. W. Brockett, "Kinematic dexterity of robot mechanisms", *Int. J. Robotics Research* **13**, No. 1, 1–15 (1994).
14. R. V. Mayorga, B. Ressa and A. K. C. Wong, "A dexterity measure for robot manipulators", *Proc. IEEE International Conference on Robotics and Automation* (1990), **Vol. 1**, pp. 656–661.
15. T. Yoshikawa, "Manipulability of robotic mechanisms", *Int. J. Robotics Research* **4**, No. 2, 3–9 (1985).
16. C. M. Gosselin and J. Angeles, "A Global performance index for the kinematic optimization of robotic manipulators", *ASME Journal of Mechanical Design* **113**, No. 3, 220–226 (1991).
17. J. Angeles and C. S. López-Cajún, "Kinematic isotropy and the conditioning index of serial robotic manipulators", *Int. J. Robotics Research* **11**, No. 6, 560–570 (1992).
18. Z. M. Bi and S.Y. T. Lang, "Joint Workspace of Parallel Kinematic Machines", *IMTI-NRC Technical Report* (London, Canada, 2004).
19. E. Kannatey-Asibu, "New concepts on multi-sensor monitoring for reconfigurable machining systems", *Proceedings of the ASME Manufacturing Science and Engineering Division ASME International Mechanical Engineering Congress and Exposition*, Anaheim, CA (1998) **Vol. 8**, pp. 589–594.
20. Suk-Hwan Suh, Yoonho Seo, So-Min Lee, Tae-Hoon Choi, Gwang-Sik Jeong and Dae-Young Kim, "Modeling and implementation of Internet-based virtual machine tool", *Int. J. Advanced Manufacturing Technology* **22**, 516–522 (2003).
21. Ji Y. Lee, Hye J. Kim and Kyo C. Kang, "A real world object modeling method for creating simulation environment of real-time systems", *Conference on Object-Oriented Programming, Systems, Languages, and Applications* (*OOPSLA*), Minneapolis, Minnesota USA (Oct. 15–19, 2000) pp. 93–103.
22. Chris Lattner and Ming-Shu Hsu, "Developing a graphical robotics simulator", *IASTED International Conference, Modeling & Simulation* (*MS'99*) http://nondot.org/sabre/Java/GRAS/GRASPaper.pdf.
23. Dongyao Wang, Sudong Ma and Xianzhong Dai, "Web-based robotic control system with flexible framework", *Proceedings of the IEEE International Conference on Robotics and Automation*, New Orleans, LA (April, 2004). pp. 3351–3358.
24. R. Marin, P. J. Sanz and A. P. Del Pobil, "Teleoperated robot system via web: the UJI telerobotic training system", *Int. J. Robotics and Automation* **17**, No. 3, 105–111 (2002).
25. Andreas Speck and Herbert Klaeren, "RoboSiM: java 3D robot visualization", *Proceedings of the IECON'99, the 26th Annual Conference of the IEEE Industrial Electronics Society*, San Jose, CA (1999) pp. 821–826.
26. D. Zhang and C. M. Gosselin, "Kinetostatic analysis and optimization of Tricept machine tools family", *ASME Journal of Manufacturing Science and Engineering* **124**, No. 3, 725–733 (2002).
27. D. Zhang, Z. Y. Xu, C. Mechefske and F. Xi, "The optimum design of parallel kinematic toolheads with genetic algorithms", *Robotica* **22**, Part 1, 77–84 (2004).
28. D. Zhang, F. Xi, C. Mechefske and Sherman Y. T. Lang, "Analysis of parallel kinematic machines with kinetostatic modelling method", *Int. J. Robotics and Computer Integrated Manufacturing* **20**, No. 2, 151–165 (2004).
29. F. Xi, D. Zhang, Z. Y. Xu and C. Mechefske, "Comparative study of Tripod-type machine tools", *Int. J. Machine Tools and Manufacture* **43**, No. 7, 721–730 (2003).
30. F. Xi, W. Han, M. Verner and A. Ross, "Development of a sliding-leg tripod as an add-on device for manufacturing", *Robotica* **18**, Part 3, 285–294 (2001).
31. Stefan Muller and Heinz Waller, "Efficient integration of real-time hardware and web-based services into Matlab" *11th European Simulation Symposium and Exhibition*, Castle, Erlangen-Nuremberg, Germany (October 26–28, 1989) http://www.held-mueller.de/JMatLink/, 1999.

https://doi.org/10.1017/S0263574705002602 Published online by Cambridge University Press